Structural Engineering and Mechanics, *Vol. 59, No. 5 (2016) 885-899*
DOI: http://dx.doi.org/10.12989/sem.2016.59.5.885

Plastic energy approach prediction of fatigue crack growth

Sofiane Maachou[1a], Abdelkader Boulenouar[*1], Mohamed Benguediab[1b],
Mohamed Mazari[1c] and Narayanaswami Ranganathan[2d]

[1]*Materials and Reactive Systems Laboratory, Mechanical Engineering Department,
University of Sidi-Bel-Abbes, BP. 89, City Larbi Ben Mhidi, Sidi Bel Abbes 22000, Algeria*
[2]*School Polytechnic University of Tours, 7 Avenue Marcel Dassault 37004 Tours, France*

(Received July 5, 2015, Revised May 25, 2016, Accepted June 28, 2016)

Abstract. The energy-based approach to predict the fatigue crack growth behavior under constant and variable amplitude loading (VAL) of the aluminum alloy 2024 T351 has been investigated and detailed analyses discussed. Firstly, the plastic strain energy was determined per cycle for different block load tests. The relationship between the crack advance and hysteretic energy dissipated per block can be represented by a power law. Then, an analytical model to estimate the lifetime for each spectrum is proposed. The results obtained are compared with the experimentally measured results and the models proposed by Klingbeil's model and Tracey's model. The evolution of the hysteretic energy dissipated per block is shown similar with that observed under constant amplitude loading.

Keywords: fatigue crack growth; variable amplitude; hysteretic energy; energy approach; aluminum alloy

1. Introduction

The fatigue crack propagation behavior of metals is known to depend upon a number of variables including the mechanical properties and microstructure, specimen size, environmental conditions and the plasticity effects at the crack tip. The vast majority of fatigue research has been concentrated on examining the phenomena under constant and variable amplitude loading using the energy approach.

The use of a cyclic plastic dissipation criterion for fatigue crack growth was first proposed by Rice (1967). From this date, plastic energy approaches to fatigue crack extension prediction have been the subject of several experimental, analytical and numerical investigations. Weertman (1973) proposed that the crack advances when the accumulated plastic energy at the crack tip reaches a critical value. (Bodner *et al.* 1983, Klingbeil 2003) has proposed a crack growth law, in which the fatigue crack growth rate was related to the total plastic energy dissipated ahead of a

∗Corresponding author, Ph.D., E-mail: aek_boulenouar@yahoo.fr
[a]Dr., E-mail: Sofiane_8381@yahoo.fr
[b]Ph.D., E-mail: benguediab_m@yahoo.fr
[c]Ph.D., E-mail: mazari_m@yahoo.fr
[d]Ph.D., E-mail: narayanaswami.ranganathan@univ-tours.fr

http://www.techno-press.org/?journal=sem&subpage=8 ISSN: 1225-4568 (Print), 1598-6217 (Online)

crack tip under cyclic loading. (Mazari *et al.* 2008, Mazari 2003) proposed an empirical correction factor which takes into account the over evaluations obtained by hysteresis loops and shows the different effects of plasticity, crack closure and opening mode. Benguediab *et al.* (2012) presents the results of a quantitative analysis of the characterized features with respect to different parameters governing the crack propagation behavior completed by an energy analysis. Khelil *et al.* (2013) proposed an approach, for the evaluation of the cyclic plastic strain energy at the crack tip in mode Shozo *et al.* (1977) measured the cyclic work to produce a unit area of fatigue crack for a steel of low carbon content and for high resistance aluminum alloys, using micro strain gages stuck in the plastic zone associated with a fatigue crack. Callaghana *et al.* (2010) investigated the energy-based approach for the evaluation of low cycle fatigue behaviour Mo steel at elevated temperature. Plastic strain energy was determined per cycle and found to characterise both crack initiation and propagation to failure regimes. Daily and Klingbeil (2006) extended the dissipated energy approach to fatigue crack growth in a homogeneous material under sustained mixed-mode loading conditions. Baudendistel and Klingbeil (2013) extended the dissipated energy theory of fatigue crack growth in ductile solids in bimaterial interface geometry under mixed-mode I/II loading, with application to fatigue debonding of layered materials. Maure *et al.* (2009) proposed a new engineering model for short crack growth under low cycle fatigue loading based on a partition of energy density into plastic distortion energy density and elastic opening energy density. Noban *et al.* (2009) investigated the different cyclic plasticity models in conjunction with the energy based-critical plane fatigue damage approach to evaluate the fatigue life of steels under various proportional and non-proportional loading conditions. Moyer and Sih (1984) proposed an accumulative damage model based on the hysteresis strain energy density for predicting fatigue crack growth. Bouchouicha *et al.* (2015) investigated the microhardness measurements to evaluate the energy at the crack tip during the propagation of a crack in a welded joint. The strain energy density approach proposed by Sih and Macdonald (1974), Sih (1974) was investigated by several authors to predict the fatigue crack growth (Sih 1974, Hachi *et al.* 2010, Balasubramanian and Guha 2000, Bian and Taheri 2011, Chang and Xu 2006). In this paper, an analysis of fatigue crack propagation based on energetic approach is proposed. An analytical model describing the material behavior is proposed for variable amplitude loading.

The present paper is organized as follows: Section 2 presents the materials and experimental procedures used in this investigation. Section 3 addresses the identification of energy parameters for constant and variable amplitude loading. Section 4 expose the analytical model proposed in this study. Finally, section 5 concludes the present investigation.

2. Materials and experimental procedures

2.1 Material

The material used in this investigation is aluminum alloy 2024 T351 whose chemical composition and the mechanical characteristics are given in Tables 1-2, respectively.

Table 1 Nominal composition (in %)

Si	Fe	Cu	Mn	Mg	Cr	Zn	Ti	Al
0.10	0.22	4.46	0.66	1.50	0.01	0.04	0.02	Remain

Table 2 Nominal mechanical properties

Mechanical properties	
Conventional yields stress at 0.2% of plastic strain $\sigma_{0.2}$ (MPa)	318
Stress at fracture σR (MPa)	524
Elongation *A*%	12.8
Strength coefficient *K* (MPa)	652
Hardening coefficient n	0.104
Cyclic yield strength (MPa)	500
Cyclic strength coefficient *K*' (MPa)	811.4
Cyclic hardening exponent *n*'	0.078

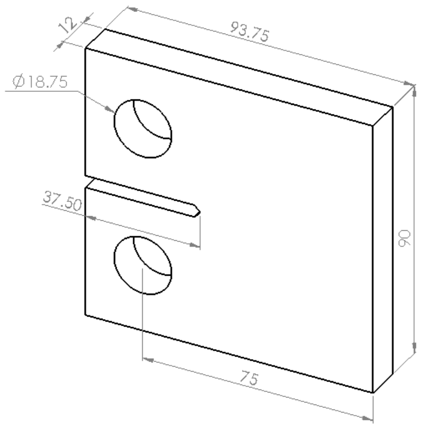

Fig. 1 CT75 specimen

2.2 Experimental procedures

In this study, the compact tension CT75 specimens with thichness *B*=12 mm and with *W*=75 mm were used in the fatigue test Fig. 1.

Crack closure was measured using the differential compliance technique. These recording were made at quasi static conditions, at a frequency of 0.05 Hz.

This technique uses the crack opening displacement (COD) response of the specimen to the variation of the far field applied load. A typical load versus COD curve can be seen in Fig. 2.

The linear relationship of load and COD represents a fully open crack. The crack is closed when no change of COD can be detected with load variation. A nonlinear relationship of load and COD indicates a partially open crack. The non-linear compliance characteristics below the first point of crack wake contact (K_I) have been confirmed by studies of stress-strain distribution of the crack tip under the effect of crack closure.

Crack closure information during constant amplitude loading (CAL) and variable amplitude loading (VAL) were obtained using the compliance technique. A crack opening displacement gauge (CODG) was used to obtain displacement data. The far field load data was obtained via the Instron control tower. The use of CODG provides the global COD of the specimen. Hence, it is expected that the crack closure level will be directly related to response of crack surfaces through

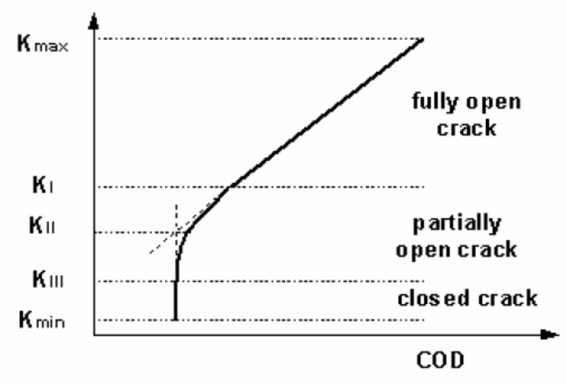

Fig. 2 Typical crack opening displacement response to far field load under the effect of crack closure

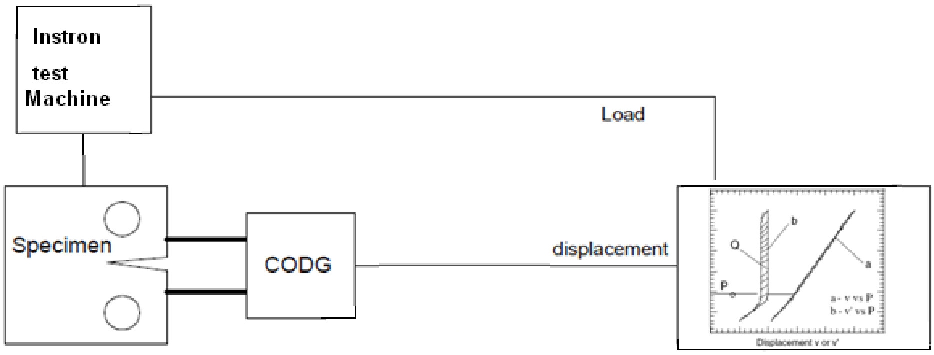

Fig. 3 Crack closure measurement system

the entire specimen thickness.

The set up of the devices used for recording of the compliance curves can be seen in Fig. 3. The applied load was acquired directly from the Instron test machine. The data acquisition card was the interface between the computer and the Instron test machine.

The tests were performed at room temperature with load ratios R=0.01, 0.1, 0.33, 0.54 and 0.7. Constant loading amplitude (CLA) tests were performed to evaluate the fatigue crack growth properties of specimens. The stress intensity factor rang ΔK for CT 75specimen is given by

$$\Delta K = \frac{\Delta P}{B\sqrt{w}} f\left(\frac{a}{w}\right) \tag{1}$$

Where w and B are respectively the width and the thickness of the specimen, a, is the crack length. In order to obtain more precision, two functions of $f(a/w)$ were used

✓ for 0.2 <a/w<0.3 (Newman 1974):

$$f(a/w) = 4.55 - 40.32(a/w) + 414.7(a/w)^2 - 1698(a/w)^3 + 3781(a/w)^4 - 4287(a/w)^5 + 2017(a/w)^7 \tag{2a}$$

✓ for 0.3 <a/w<0.7 Srawley and Gross (1972):

$$f(a/w) = 29.6(a/w)^{0.5} - 185.5(a/w)^{1.5} - 655.7(a/w)^{2.5} - 1017(a/w)^{3.5} + 638.9(a/w)^{4.5} \qquad (2b)$$

For the variable amplitude loading (VLA), the tests were performed at room temperature with four types of spectrum loads Fig. 4. These spectrums (blocks) are defined as:

- ✓ Spectrum A: consists of several load excursions which have a probability of one cycle per flight. This spectrum represents the most probable GAG cycle (Ground Air Ground) and consists of four mean levels.
- ✓ Spectrum B: consists of 10 cycles in the first three load and two cycles in the fourth level.
- ✓ Spectrum C and D: are similar to Spectrum B. with 50 and 100 cycles in the high load level.

Table 3 illustrated the type of blocks and the loading conditions used in this investigation. N_i (i=1..4) represents the number of cycle per level.

The global hysteresis energy Q was measured by amplifying the load P versus displacement v diagram measured under the loading axis. Examples of the nominal and amplified load displacement diagrams are given in Fig. 5 and the different parameters measured are indicated, for the case of variable amplitude loading (VLA). The crack opening level is determined from the differential crack opening v_o versus the load diagrams, using the Kikukawa (1976) technique

$$v' = v - \alpha P \qquad (3)$$

where v is the crack mouth opening displacement measured under the loading line; α, the maximum specimen compliance; P, the load and P_o, the crack opening load.

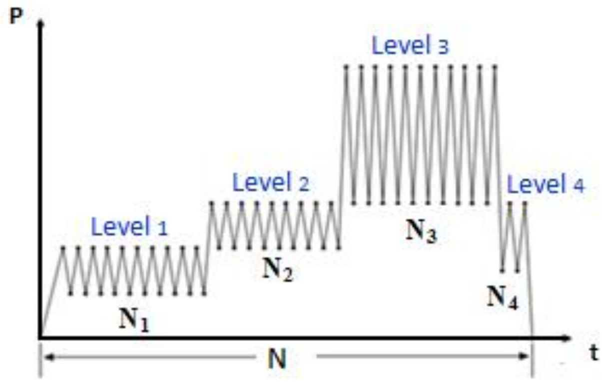

Fig.4 Configuration of different block load tests

Table 3 Condition of loading for the spectrum

Type of Block	P_{min}=80 daN P_{max}=150 daN R=0.53	P_{min}=160 daN P_{max}=392 daN R=0.41	P_{min}=323 daN P_{max}=600 daN R=0.54	P_{min}=138 daN P_{max}=323 daN R=0.43
	N1	N2	N3	N4
A	1	1	1	1
B	10	10	10	2
C	10	10	50	2
D	10	10	100	2

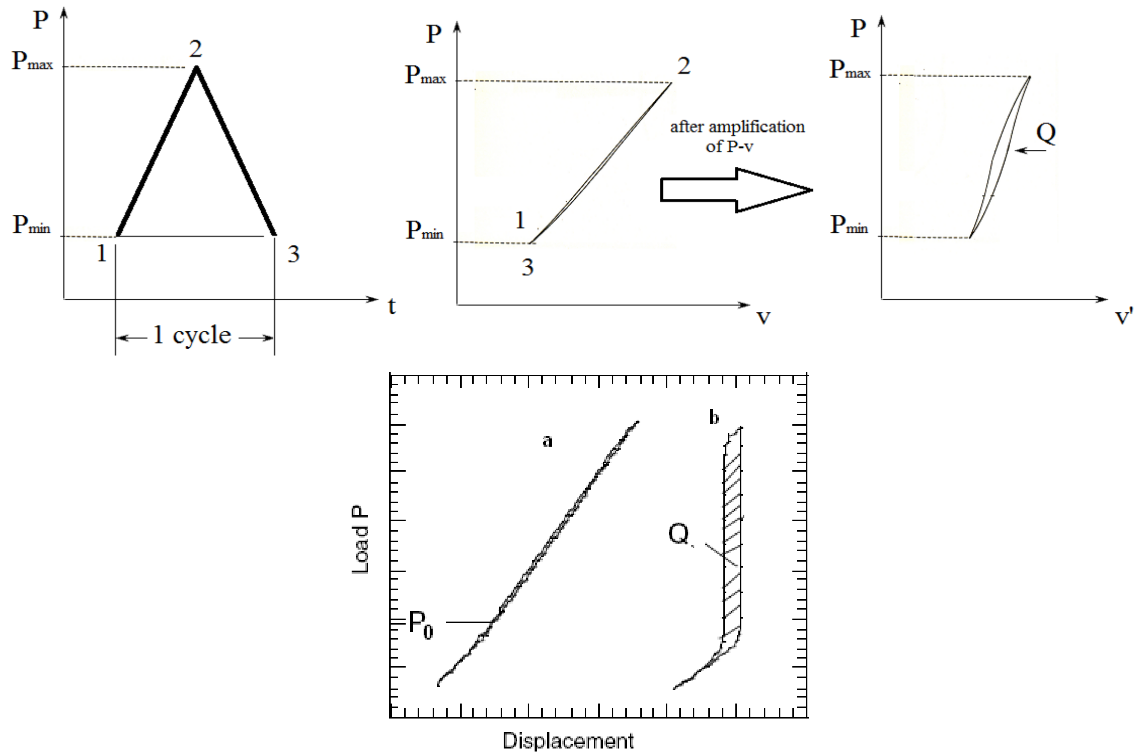

Fig. 5 Load versus displacement diagrams and measurement of hysteresis energy: CAL condition For a crack length given at a frequency of 0.05 Hz, and after amplification

Hysteresis energy, Q, was measured by numerically integrating the area under the load versus (amplified) displacement diagrams measured under the loading line of the specimen (Mazari *et al*. 2008, Benguediab *et al*. 2012, Ranganathan *et al*. 2008, Ranganathan *et al*. 1987, Ranganathan 1999).

For the variable amplitude loading (VAL), we consider two cases:

• **Case 1**: The crack advance is negligible during a block Fig. 6(a). Then we regard total energy Q_T as the energy of the envelope Q_{env} and the elementary energies Q_i associated with each individual cycle as (Benguediab 1989)

$$Q_{Total} = Q_{env.} + \sum Q_i \tag{4}$$

With: $Q_{env}=Q_1+Q_3+Q_6+Q_8+Q_{10}$

• **Case 2**: There are appreciable advance of the crack during each block Fig. 6(b). In this case we consider that the energies dissipated in each individual cycle Q_i as

$$Q_{Total} = \sum Q_i \tag{5}$$

The analysis consider that, in the first case, the crack is almost stationary during the block of the charge; all hysteretic energy is dissipated in the same plastic zone. Whereas in the second case, the energy of plastification is integrated at advanced crack with each cycle.

(a) Spectrum A (Case 1) (b) Spectrum C (Case 2)

Fig. 6 Diagram for VAL condition (Benguediab 1989)

Table 4 Cyclic plastic strain energy parameters

$\Delta\sigma_0$	$\Delta\varepsilon_0$	αM	N'	N"	Integral	$\Delta W/\Delta K4$
914	0.0111	6.67E-4	0.148	0.078	0.0138	2.92E-13

3. Resultants and discussion

3.1 Constant amplitude loading condition

An analytical estimation of energy dissipated ΔW in the plastic zone has been made based on a model developed by Tracey (1971) using

$$\Delta W = 2(1-N'')\frac{1-N''}{1+N''}\Delta\sigma_0 . \Delta\varepsilon_0 \left(\frac{\Delta K_I}{\Delta\sigma_0}\right)^4 \int_0^{\pi/2} f_N(\theta)^2 d\theta \tag{6}$$

$f_N(\theta)$ is a dimensionless function which defines the profile of iso-deformation as a function of polar coordinates at the crack tip. N" is the exponent linking the stress amplitude $\Delta\sigma$ and the plastic strain amplitude $\Delta\varepsilon_p$. $\Delta\sigma_0$ and $\Delta\varepsilon_0$ related to the cyclic stress-strain law Khelil *et al.* (2013).

Several authors are investigated Eq. (6) to analyse the fatigue crack propagation based on plastic energy approach (Mazari 2003, Khelil *et al.* 2013). The results obtained after the identification of the cyclic plastic strain energy parameters are summarized in Table 4.

The total dissipated energy Q in the specimen is given by

$$Q = \Delta W . B \tag{7}$$

Using the results of Table 4, the relationship between the plastic energy Q and ΔK is given by

$$Q = 2.976 \ . \ 10^{-7} \ \Delta K^4 \tag{8}$$

Q is expressed in J/m and ΔK in MPa m$^{0.5}$.

3.2 Variable amplitude loading condition

In this section, we present the procedures analytical and experimental to determine the

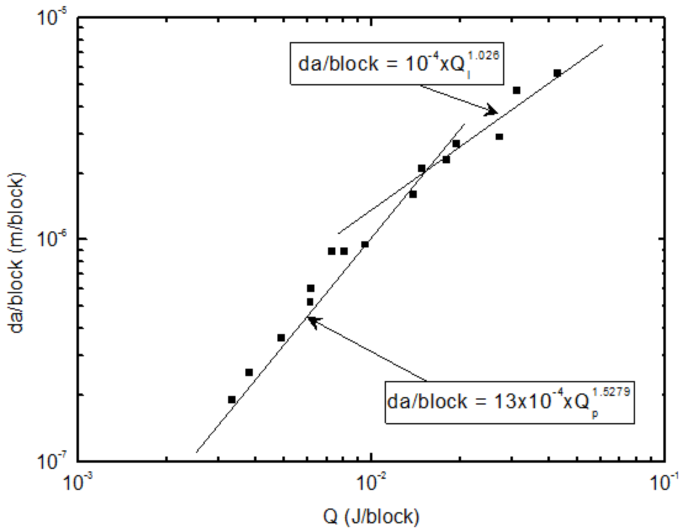

Fig. 7 Evolution of the crack growth rate da/block vs. the energy dissipated per cycle ΣQ_i, for block A

relationship between the crack growth da/block and the energy Q. In what follows, the steps to determine the relation between the crack growth da/block and the energy Q are presented only for a block (block A, for example).

The evolution of the crack growth rate with respect to the energy dissipated per cycle Q for block A is presented in Fig. 7. In this figure, we show the existence of two distinct stages.

✓ For lower growth rates values, the relationship between da/dN and Q can represent by a power law of the type Eq. (9a)

$$\left(\frac{da}{block}\right)_p = B \times Q_p^n \tag{9a}$$

$$\left(\frac{da}{block}\right)_p = 13 \times 10^{-4} \times Q_p^{1.5279} \tag{9b}$$

Where Q_p is the power part of Q; n is an exponent.

✓ For the growth rate higher than 1.6×10-6 m/block the energy dissipated per cycle is linear and can be expressed as follow Eq. (10a)

$$\left(\frac{da}{block}\right)_l = A \times Q_l \tag{10a}$$

$$\left(\frac{da}{block}\right)_l = 10^{-4} \times Q_l^{1.026} \tag{10b}$$

Where Q_l is a linear form of Q.

Considering that, there is a continuity of the growth rate of the crack to the transitions. This continuity lets equalize Eqs. (9) and (10) which give

$$A \times Q_l = B \times Q_p^n \tag{11}$$

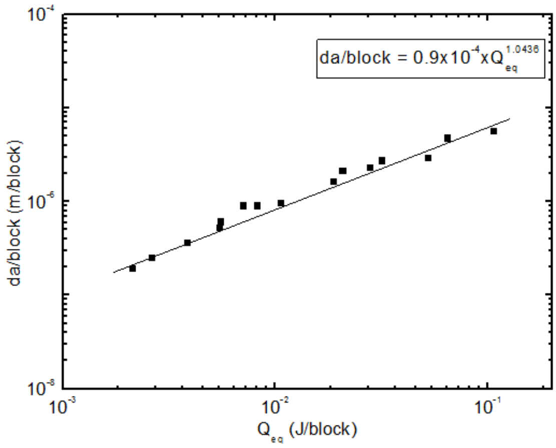

Fig. 8 Evolution of da/block vs. Q_{eq} for block A after correction

Thus

$$Q_l = \frac{B}{A} \times Q_p^n \tag{12}$$

Mazari *et al.* (2008), Mazari (2003) used this technique to determine la relationship between da/dN and Q in the case of fatigue crack growth under constant amplitude loading.

The equivalent energy dissipated by Q_{eq} cycle has the form

$$Q_{eq} = M \times Q_p^n \tag{13}$$

With: $M = \dfrac{B}{A}$

Using Eq. (13), the equivalent energy dissipated per cycle Q_{eq} has the form

$$Q_{eq} = 13 \times Q_p^{1.5279} \tag{14}$$

The evolution of the crack growth rate with respect to the energy dissipated per cycle Q for block A

The evolution of the crack growth rate da/block with respect to the equivalent energy dissipated per cycle Q_{eq} is presented in Fig. 8. In this figure, we show that this evolution presents a linear relation given by

$$\frac{da}{block} = 0.9 \times 10^{-4} \times Q_{eq}^{1.0436} \tag{15}$$

The same energetic analysis was applied for the other blocks (B, C and D). We obtained the following relation

Block B: $$\frac{da}{block} = 3 \times 10^{-4} \times Q_{eq}^{1.0607} \tag{16}$$

Block C: $$\frac{da}{block} = 1 \times 10^{-4} \times Q_{eq}^{0.8443} \tag{17}$$

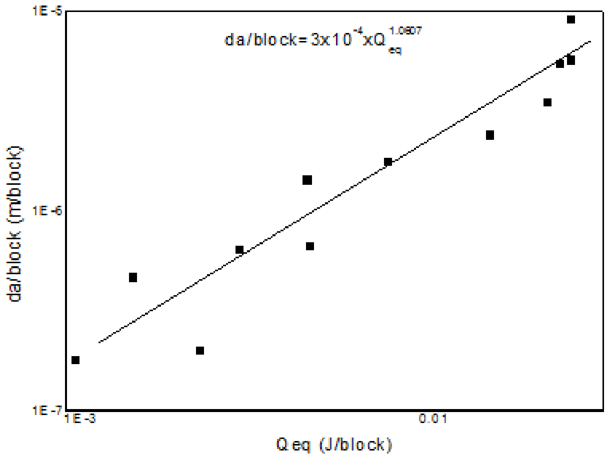

(a) for Block B

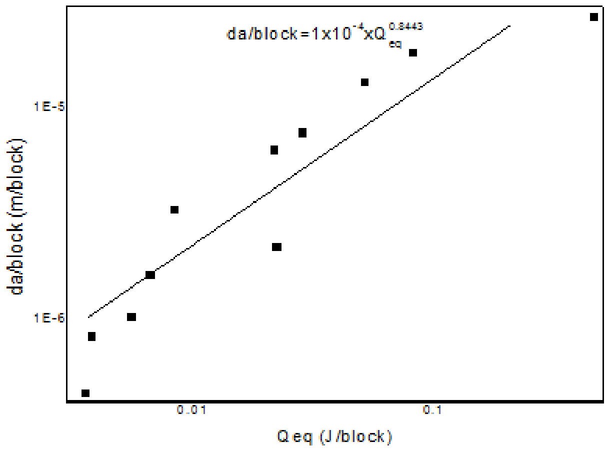

(b) for Block C

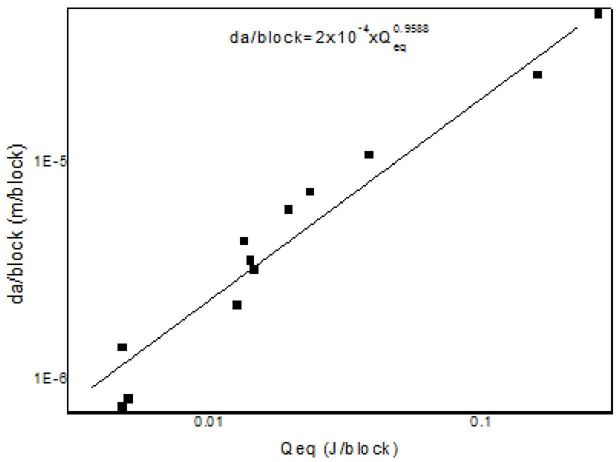

(c) for Block D

Fig. 9 Evolution of da/block vs Q_{eq}

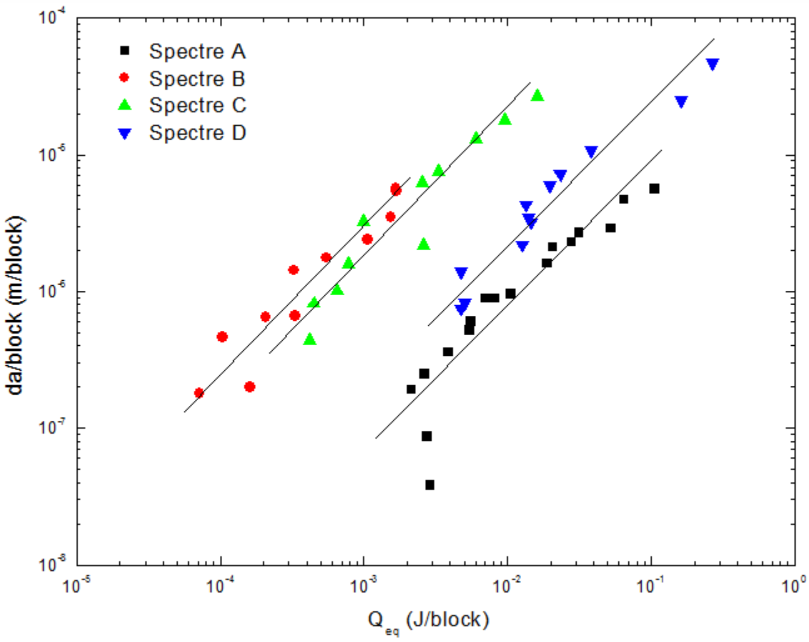

Fig. 10 Evolution of da/block with respect to Q_{eq}

Block D: $$\frac{da}{block} = 2\times10^{-4}\times Q_{eq}^{0.9588} \tag{18}$$

Figs. 9(a)-(b)-(c) expose the evolution of da/block vs Q_{eq} for block B, C and D respectively.

The evolution of da/block vs. the equivalent energy Q_{eq} for the four blocks is illustrated in Fig. 10.

4. Proposed model

In this section, we proposed an analytical model to estimate a lifetime needed to advance a crack length a=54 mm (with a_0=24 mm), for each spectrum. The crack propagation (da/block) is characterized by successive propagation steps under variable amplitude loading. Each step consists of:

1. Input the geometric parameters and the material properties data of the problem.
2. Calculation of $f(a/w)$ using Eq. (2a) or (2b).
3. Choosing the block type.
4. Evaluation of K_{max} and ΔK.
5. Evaluation of Q_{eq}.
6. Calculation of crack increment length Δa.
7. Estimation of crack propagation rate (da/block)
8. Calculation of new crack tip position (with $a=a_0+\Delta a$).
9. Crack arrests (if a=52 mm)? If yes, go to step 10. If no, go to step 11.
10. Stop

11. Return to step 3-9

Fig. 11 shows the Flow-chart of the prepared MATLAB code based on the combination of the mathematical calculation and the plastic energy approach prediction of fatigue crack growth.

✓ The results of the proposed model are compared with the experimentally measured results and the models proposed by Tracey's (1971) model and Klingbeil's (2003) model. The relationship between da/block and energy hysteretic dissipated Q proposed by Tracey (1971) and Klingbeil (2003) are given by Eqs. (19) and (20), respectively. Table 5 shows the number of blocks (lifetime) calculated for each block using four approaches.

$$\frac{da}{block} = 5.811 \times 10^{-4} \times Q^{1.05} \tag{19}$$

$$\frac{da}{block} = 1.856 \times 10^{-4} \times Q^{1.05} \tag{20}$$

• The results obtained by our model give a number of the blocks acceptable for the spectrum (A) with an error of 9.04% to that obtained by Eq. (15).

• For the spectrum B, the analytical model presents an error of 53.15% compared to that obtained experimentally. This value represents half of lifespan obtained by the experimental approach.

• In the case of spectrum C, the comparison between the analytical model and experimental results gives a calculation error that exceeds 16%.

• In the case of the spectrum D, the resulting calculation showed that the number of blocks is less than that measured experimentally. This difference presents an error 33.27%.

✓ The number of block estimated by Tracey's model presents an error varied between 75.7 and 85.5% comparatively to the experimental results.

✓ The Klingbeil's model lead generally to a stable error for spectra B, C and D. In the case of spectrum A, the number of the blocks exceeds the half number of blocks measured experimentally.

Table 5 Number of blocks comparison

Blocks	Number of blocks		Error l%l
A	Measured	75120	9.04
	Proposed model	68323	/
	Tracey	10880	85.5
	Klingbeil	34058	54.7
B	Measured	23900	53.15
	Proposed model	11196	/
	Tracey	5599	76.6
	Klingbeil	17524	26.7
C	Measured	9600	16.17
	Proposed model	11153	/
	Tracey	2315	75.9
	Klingbeil	7242	24.6
D	Measured	5500	33.27
	Proposed model	3670	/
	Tracey	1336	75.7
	Klingbeil	4179	24.0

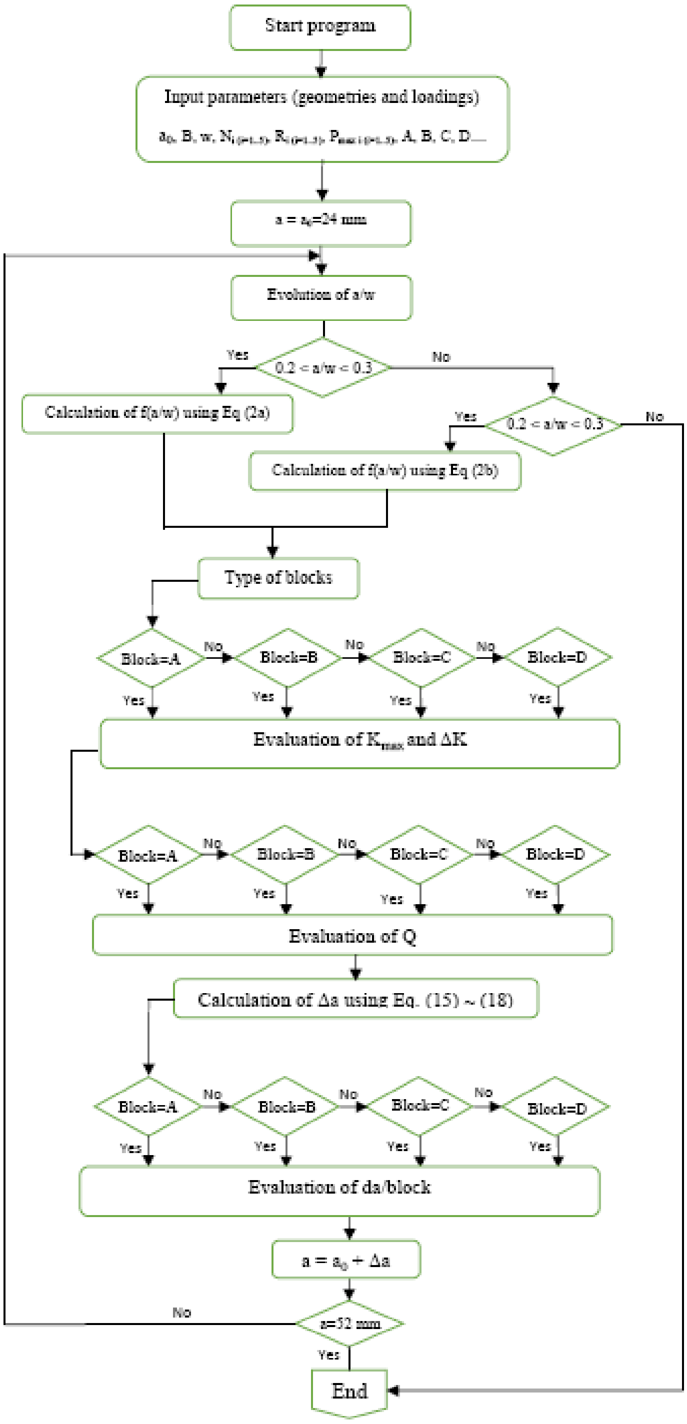

Fig. 11 Flow chart of the numerical process

5. Conclusions

Plasticity effects at the crack tip had been recognized as ‘‘motor’’ of crack propagation. The growth of cracks is related to the existence of a crack tip plastic zone, whose formation and intensification is accompanied by energy dissipation. In this paper, the fatigue crack propagation under variable amplitude loading analyses based on plastic energy approach has been investigated on aluminum alloy 2024-T351. The linear relation between the crack growth rate da/block the equivalent energy dissipated per cycle Q_{eq} is presented for different block load tests. The results obtained for proposed model are compared with the experimentally measured results and the models proposed by Klingbeil’s model and Tracey’s model. The results obtained by the analytical model give acceptable results compared to the results found by two models studied.

References

Balasubramanian, V. and Guha, B. (2000), “Fatigue life prediction of welded cruciform joints using strain energy density factor approach”, *Theor. Appl. Fract. Mech*., **34**(1), 85-92.

Baudendistel, C.M. and Klingbeil, N.W. (2013), “Effect of a graded layer on the plastic dissipation in mixed-mode fatigue crack growth along plastically mismatched interfaces”, *Int. J. Fatig.*, **51**, 96-104.

Benguediab, M. (1989), “Etude de la propagation des fissures de fatigue sous spectres de chargement réduits”, PhD Dissertation, Université de Poitiers, France.

Benguediab, M., Bouchouicha, B., Zemri, M. and Mazari, M. (2012), “Crack propagation under constant amplitude loading based on an energetic parameters and fractographic analysis”, *Mater. Res.*, **15**(4), 544-548.

Bian, L. and Taheri, F. (2011), “A proposed maximum ratio criterion applied to mixed mode fatigue crack propagation”, *Mater. Des.*, **32**(4), 2066-2072.

Bodner, S.R., Davidson, D.L. and Lankford, J. (1983), “A description of fatigue crack growth in terms of plastic work”, *Eng. Fract. Mech.*, **17**(2), 189-191.

Bouchouicha, B., Zemri, M., Zaim, A. and Ould Chikh, B. (2015), “Estimation of the energy of crack propagation in different zones of a welded joint by the local technique”, *Int. J. Fract.*, **192**(1), 107-116.

Callaghana, M.D., Humphries, S.R., Law, M., Ho, M., Bendeich, P., Lia, H. and Yeung, W.Y. (2010), “Energy-based approach for the evaluation of low cycle fatigue behaviour of 2.25Cr-1Mo steel at elevated temperature”, *Mater. Sci. Eng*., **527**(21-22), 5619-5623.

Chang, J., Xu, J.Q. and Mutoh, Y. (2006), “A general mixed-mode brittle fracture criterion for cracked materials”, *Eng. Fract. Mech.*, **73**(9), 1249-1263.

Daily, J.S. and Klingbeil, N.W. (2006), “Plastic dissipation in mixed-mode fatigue crack growth along plastically mismatched interfaces”, *Int. J. Fatig.*, **28**(12), 1725-1738.

Hachi, B.K., Belkacemi, Y., Rechak, S., Haboussi, M. and Taghite, M. (2010), “Fatigue growth prediction of elliptical cracks in welded joint structure: Hybrid and energy density approach”, *Theor. Appl. Fract. Mech*., **54**(1), 11-18.

Khelil, F., Aour, B., Belhouari, M. and Benseddiq, N. (2013), “Modeling of Fatigue Crack Propagation in Aluminum Alloys Using an Energy Based Approach”, *Eng. Tech. Appl. Sci. Res.*, **3**(4), 488-496.

Kikukawa, M., Jono, M., Tanaka, K. and Takatani, M. (1976), “Measurement of fatigue crack propagation and crack closure at low stress intensity level by unloading elastic compliance method”. *J. Soc. Matl. Sci. Japan*, **25**(276), 899-903.

Klingbeil, N.W. (2003), “A total dissipated energy theory of fatigue crack growth in ductile solids”, *Int. J. Fatig.*, **25**(2), 117-128.

Maurel, V., Rémy, L., Dahmen, F. and Haddar, N. (2009), “An engineering model for low cycle fatigue life based on a partition of energy and micro-crack growth”, *Int. J. Fatig.*, **31**(5), 952-961.

Mazari, M. (2003), “Contribution à l’étude d’une approche énergétique de la propagation des fissures de fatigue”, PhD Dissertation, Université de Sidi Bel Abbès, Algérie.

Mazari, M., Bouchouicha, B., Zemri, M., Benguediab, M. and Ranganathan, N. (2008), “Fatigue crack propagation analyses based on plastic energy approach”, *Comp. Matls. Sci*., **41**(3), 344-349.

Moyer, E.T. and Sih, G.C. (1984), “Fatigue analysis of an edge crack specimen: hysteresis strain energy density”, *Eng. Fract. Mech*., **19**(2), 643-652.

Newman, J.C. (1974), “Stress analysis of the compact specimen including the effects of pin loading”, *Proceedings of the National Symposium on Fracture Mechanics*, Philadelphia, August.

Noban, T.M., Jahed, H. and Varvani-Farahani, A. (2012), “The choice of cyclic plasticity models in fatigue life assessment of 304 and 1045 steel alloys based on the critical plane-energy fatigue damage approach”, *Int. J. Fatig.*, **43**, 217-225.

Ranganathan, N. (1997), “Analysis of fatigue crack growth in terms of crack closure and energy”, *Proceedings of the 2nd Symposium on Advances in Fatigue Crack Closure Measurement and Analysis,* San Diego, November.

Ranganathan, N., Chalon, F. and Meo, S. (2008), “Some aspects of the energy based approach to fatigue crack propagation”, *Int. J. Fatig.*, **30**(10-11), 1921-1929.

Ranganathan, N., Jendoubi, K., Benguediab, M. and Petit, J. (1987), “Effect of R ratio and ΔK level on the hysteretic energy dissipated during fatigue crack propagation”, *Scripta Metall.*, **21**(8), 1045-1049.

Rice, J.R. (1967), “The mechanics of crack tip deformation and extension by fatigue”, *Fatigue Crack Growth, Special Technical Publication 415. American Society for Testing and Materials*, Philadelphia, 247-311.

Shozo, I., Yoshito, I. and Fine, M.E. (1977), “Plastic work during fatigue crack propagation in a high strength low alloy steel and in 7050 AL-Alloy”, *Eng. Fract. Mech.*, **9**(1), 123-136.

Sih, G.C. (1974), “Strain energy density factor applied to mixed mode crack problems”, *Int. J. Fract.*, **10**(3), 305-321.

Sih, G.C. and Macdonald, B. (1974), “Fracture mechanics applied to engineering problems-strain energy density fracture criterion”, *Eng. Fract. Mech*., **6**(2), 493-507.

Srawley, J.E. and Gross, B. (1972), “Stress intensity factors for bend and compact specimens”, *Eng. Fract. Mech*., **4**(3), 587- 589.

Tracey, D.M. (1971), “Finite element for determination of crack tip elastic stress intensity factor”, *Eng. Fract. Mech*., **3**(3), 255-265.

Weertman, J. (1973), “Theory of fatigue crack growth based on a BCS crack theory with work hardening”, *Int. J. Fract*., **9**(2), 125-131.

CC